ERJ
Engineering Research Journal
Faculty of Engineering
Minoufiya University

# ROBUST CHATTER-FREE SLIDING MODE OBSERVER OF SENSORLESS INDUCTION MOTOR DRIVES

M. M. Mahmoud M. Khater

*Department of Electrical Engineering, Faculty of Engineering, Minoufiya University, Shebin El-Kom, Egypt*

## ABSTRACT

Sliding mode observer with its salient features is considered one of the robust observers for flux and speed estimation of sensorless induction motor drives. However, the discontinuous switching function of the sliding mode observer causes a significant chattering which is considered a serious drawback. In this paper, a modified robust chatter-free sliding mode observer for sensorless induction motor drives is presented. The discontinuous switching function is replaced by a continuous one to eliminate chattering. The accuracy and robustness of the proposed sliding mode observer are examined at motor starting and load torque variations. A floating-point Digital Signal Processor (DSP) TMS320C31 control board with a hardware/software interface is used to implement the proposed sliding mode observer for speed estimation. Simulation and experimental results are presented and discussed.

يعتبر المراقب ذو النمط الانزلاقي من الأنظمة عالية المتانة في تحسس واستشعار الفيض المغناطيسي والسرعة في نظم تسيير المحرك التأثيري. وبالرغم من هذه الصفة المميزة له إلا أنه من الأنظمة ذات التشغيل المتقطع التي بها قدر كبير من الاهتزاز والتذبذب في إشارة السرعة المستشعرة والذي يعتبر من العيوب الخطيرة في هذا النظام. يقدم هذا البحث نوعا معدلا للمراقب ذي النمط الانزلاقي يخلو من ظاهرة التذبذب والاهتزاز وذلك باستبدال دالة التشغيل المتقطعة بأخرى متواصلة، وقد تم اختبار دقة ومتانة المراقب المقترح في تحسس واستشعار سرعة المحرك التأثيري عند حالات التشغيل المختلفة، وقد تم تنفيذ هذا النظام المقترح باستخدام معالج الإشارات الرقمية، ويقدم البحث عرضا ومناقشة للنتائج التحليلية والمعملية.

***Keywords:*** Chattering, Sliding Mode Observer, Speed Sensorless

## 1. INTRODUCTION

Accurate speed information is always necessary to realize high performance and high-precision speed control of induction motor drives. Speed feedback can be achieved by using mechanical sensors such as resolvers or pulse encoders. The use of such direct sensors besides being bulky, adds an extra cost and the drive system becomes expensive. For this reason, the development of alternative indirect methods became an interesting research topic. Many advantages are expected from speed-sensorless induction motor drives such as reduced hardware complexity and lower cost, reduced size of the drive machine, elimination of the sensor cable, better noise immunity, increased reliability and less maintenance requirements. Operation in hostile environments mostly requires a motor without speed sensor [1].

Recently, serious attempts to eliminate direct speed sensor of induction motor drives are reported [2-9]. All these attempts employ motor terminal variables and its parameters, in some way or another, to estimate the speed. The question always arises is *to which extent the method is successful without degrading the dynamic performance.*

Some speed estimation methods like Model Reference Adaptive System (MRAS) methods [2], Extended Kalman Filter (EKF) algorithms [3] and adaptive flux observers [4] have been proposed in literature. These methods exhibit accurate and robust speed estimation performance; however, they are highly dependent on the machine parameters. The induction motor is a highly coupled, nonlinear dynamic plant, and its parameters vary with time and operating conditions. Therefore, it is very difficult to obtain good performance for an entire speed range and transient states using the previous methods.

The aforementioned methods are less accurate at low speed and completely fail at standstill. For this range of operation, magnetic saliency-based speed estimation approaches are more suitable. These approaches are independent of motor parameters; however, they need a high precision measurement and increase the hardware/software complexity [1].

Alternative speed estimation methods based on artificial intelligence techniques are proposed for sensorless induction motor drives [5]. These methods may achieve robustness and high performance with parameter variations; however they are relatively complicated and require large computational time.

Recently, there is a growing interest of speed estimation methods using Sliding Mode Observer (SMO) technique based on Variable Structure Control (VSC) theory. This speed estimation technique is one of the effective methods to overcome the short comings of the previous methods. It offers many good properties, such as good performance against un-modeled dynamics, insensitivity to parameters variations, external disturbance rejection and fast dynamic response [6-9].

The design procedure of a VSC consists of two steps. *First*, a sliding surface is selected such that the desired system dynamics are achieved. *Second*, a discontinuous switching control law is defined such that any states outside the surface are driven to reach the surface in finite time (reaching mode). Once the states reach the switching surface, they are supposed to remain on this surface and slide towards the desired position (sliding mode). However, the discontinuous nature of the switching function alters the real trajectory such that it oscillates around the switching surface as shown in Fig.1.

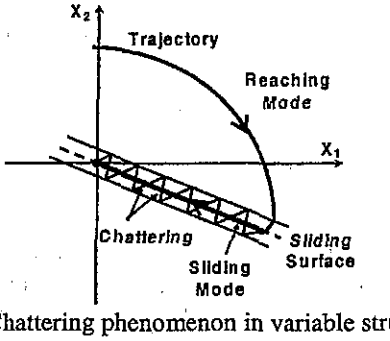


**Fig. 1** Chattering phenomenon in variable structure control (VSC)

Principally, VSC systems assume an instantaneous switching from one value to another. However, it is practically impossible to achieve such instantaneous switching necessary for VSC designs. The main reason is the existence of a finite time delay due to many factors such as control computation, limitations of physical actuators and measuring sensors, and idle times of power electronic switches. Since it is impossible to switch the control at an infinite rate, oscillation or *chattering* always occurs in the sliding mode of a VSC system [10-11].

The chattering exists in the SMO as an inherent problem associated with VSC theory. The negative side effect of chattering is that it involves high gain control action and may excite un-modeled dynamics. Thus, chatter-free becomes essential for a good performance SMO. Many research works are devoted to alleviate or remove undesirable chattering [10-13]. Chattering elimination philosophy is based on converting the discontinuous switching function to a continuous one. This is usually done by different approaches, like introducing a thin boundary layer neighboring the switching surface, using a saturation switching function to replace the discontinuous one, or using equivalent control approach.

In this paper, a robust chatter-free SMO is applied for speed estimation of sensorless induction motor drive. The speed estimation algorithm which is based on Lyapunov theory is derived and implemented. The discontinuous switching function of SMO is replaced by a continuous one using sigmoid switching function. The performances of the proposed sigmoid, chatter-free SMO, as well as the original discontinuous one, are investigated by simulation and experimentation. The results show the robustness and superiority of the proposed system.

## 2. INDUCTION MOTOR MODEL

The induction motor can be represented by its dynamic model expressed in the stationary reference frame in terms of the stator current and rotor flux as follows;

$$\frac{di_s^s}{dt} = \frac{1}{\sigma L_s}\left( u_s^s - R_s i_s^s - \frac{L_m}{L_r}\frac{d\lambda_r^s}{dt} \right) \quad (1)$$

$$\frac{d\lambda_r^s}{dt} = \frac{L_m}{T_r} i_s^s - \left( \frac{1}{T_r} - J\omega_r \right)\lambda_r^s \quad (2)$$

By considering the rotor speed as a system parameter; the dynamic model can be described by the following state equation;

$$\frac{d}{dt}\begin{bmatrix} i_s^s \\ \lambda_r^s \end{bmatrix} = \begin{bmatrix} a_{11} & a_{12} \\ a_{21} & a_{22} \end{bmatrix}\begin{bmatrix} i_s^s \\ \lambda_r^s \end{bmatrix} + \begin{bmatrix} b_1 \\ 0 \end{bmatrix}\begin{bmatrix} u_s^s \end{bmatrix} = Ax + Bu_s \quad (3)$$

where $a_{11}$, $a_{12}$, $a_{21}$, $a_{22}$ and $b_1$ are given in the Appendix. The electromechanical equation is given by;

$$J\frac{d\omega_r}{dt} = T_e - T_L - B\omega_r \quad (4)$$

where the electromagnetic torque is expressed as;

$$T_e = \frac{2}{3}\frac{L_m}{L_r}\left[ \lambda_{dr}^s i_{qs}^s - \lambda_{qr}^s i_{ds}^s \right] \quad (5)$$

## 3. DESIGN OF SLIDING MODE OBSERVER

With reference to the induction motor model and considering the stator currents as the system outputs,

the SMO for rotor flux estimation can be constructed as [9]:

$$p\hat{x} = A\hat{x} + Bu_s + K_1 \ \mathrm{sgn}\left(\hat{i}_s^s - i_s^s\right) \quad (6)$$

Where $K_1$ is a gain matrix which can be arranged in the following general form;

$K_1 = [K \ \ -K]^T$, $K = kI$ and k is the switching gain.

The error equation which takes into account the parameter variation can be expressed by subtracting Eqn. (3) from Eqn. (6):

$$pe = Ae + \Delta A\hat{x} + K_1 \,\mathrm{sgn}\left(\hat{i}_s^s - i_s^s\right) \quad (7)$$

where;

$$e = \hat{x} - x = [e_i \ \ e_\lambda]^T,\ e_i = \hat{i}_s^s - i_s^s,\ e_\lambda = \hat{\lambda}_r^s - \lambda_r^s$$

and $\Delta A = \begin{bmatrix} \Delta a_{11} & \Delta a_{12} \\ \Delta a_{21} & \Delta a_{22} \end{bmatrix}$

Defining the switching surface S of SMO as:

$$S(t) = e_i = \hat{i}_s^s - i_s^s = 0 \quad (8)$$

The sliding mode occurs when the following sliding condition is satisfied;

$$e_i^T \cdot pe_i < 0 \quad (9)$$

Since the sliding mode condition is satisfied with a small switching gain k, then

$$e_i^T = pe_i = 0 \quad (10)$$

From which,

$$0 = a_{12}e_\lambda + \Delta a_{11}\hat{i}_s^s + \Delta a_{12}\hat{\lambda}_r^s - L \quad (11)$$

$$pe_\lambda = a_{22}e_\lambda + \Delta a_{21}\hat{i}_s^s + \Delta a_{22}\hat{\lambda}_r^s + L \quad (12)$$

where, $L = -K \,\mathrm{sgn}\left(\hat{i}_s^s - i_s^s\right)$

From Eqns. (11) and (12), the error equation for the rotor flux in sliding mode condition is obtained as;

$$pe_\lambda = (a_{22} + a_{12})e_\lambda + (\Delta a_{21} + \Delta a_{11})\hat{i}_s^s + (\Delta a_{22} + \Delta a_{12})\hat{\lambda}_r^s \quad (13)$$

### 3.1. Rotor Speed Estimation Algorithm

If the rotor speed is considered as a variable parameter assuming no other parameter variations, the matrix $\Delta A$ is expressed as follows:

$$\Delta a_{11} = 0,\ \Delta a_{12} = \frac{-\Delta\omega_r J}{\varepsilon},\ \Delta a_{21} = 0,\ \Delta a_{22} = \Delta\omega_r J,\ \Delta\omega_r = \hat{\omega}_r - \omega_r$$

From Eqn. (13), the error equation of the rotor flux observer in sliding mode condition becomes:

$$pe_\lambda = (a_{22} + a_{12})e_\lambda + (I - I/\varepsilon)J\Delta\omega_r\hat{\lambda}_r^s \quad (14)$$

The Lyapunov function candidate is chosen as;

$$V = e_\lambda^T e_\lambda + \frac{1}{\mu\varepsilon}\Delta\omega_r^2, \quad \mu > 0 \quad (15)$$

where $\mu$ is a positive constant.

The Lyapunov function must be determined in order to assure the convergence of parameter estimation according to the Lyapunov stability theory.

The time derivative of V can be expressed as;

$$pV = pV_1 + pV_2 \quad (16)$$

where,

$$pV_1 = L^T\Lambda^T a_{12}^{-1}L \quad (17)$$

$$pV_2 = L^T\Lambda^T a_{12}^{-1}\frac{\Delta\omega_r}{\varepsilon}J\hat{\lambda}_r^s + \frac{2}{\mu\varepsilon}\Delta\omega_r\frac{d}{dt}\hat{\omega}_r \quad (18)$$

and $\Lambda = I - \varepsilon I$

The condition of (16) being negative definite will be satisfied if $pV_1 < 0$ and $pV_2 = 0$.

The condition $\rho V_1 < 0$ is satisfied by choosing

$$\Lambda^T = -\gamma a_{12}, \qquad \gamma > 0 \quad (19)$$

where $\gamma$ is a positive constant.

With this assumption, the condition $\rho V_2 = 0$ gives

$$p\hat{\omega}_r = \mu\gamma L^T J\hat{\lambda}_r^s \quad (20)$$

This equation can be written for the speed estimation in the following form:

$$\hat{\omega}_r = \mu\gamma k\int\left[\mathrm{sgn}\left(\hat{i}_{ds}^s - i_{ds}^s\right)\cdot\hat{\lambda}_{qr}^s - \mathrm{sgn}\left(\hat{i}_{qs}^s - i_{qs}^s\right)\cdot\hat{\lambda}_{dr}^s\right]dt \quad (21)$$

Figure 3 shows the block diagram of the proposed SMO. It is composed of two parts; a sliding mode observer for rotor flux estimation and a sliding mode speed estimation algorithm.

## 4. SIGMOID CHATTER-FREE FUNCTION

As it has been stated earlier, chattering is the main drawback of the SMO due to its discontinuous switching nature. This phenomenon is undesirable because it may excite the high frequency un-modeled dynamics of potential unforeseen instability, and can also cause serious damage to actuators or the plant. Chattering elimination is based on converting the discontinuous switching function to a continuous one. Different approaches are proposed by literature, like introducing a thin boundary layer neighboring the switching surface, using a saturation switching function to replace the discontinuous one or using equivalent control approach **[10-13]**. The boundary layer approach can give a chatter-free system, but a finite steady-state error would exist. Hence, to eliminate the chattering, most of approaches use the saturation function to replace the sign one. The sigmoid function represents saturation effect; however it is smooth and completely continuous function. The present work proposes the sigmoid switching function to represent a more smooth action that would maintain the state trajectories of the system on the sliding surface S. The sigmoid function (Fig. 2(a)) is described by;

$$\text{tansig} = \frac{2}{1+e^{-2n}} - 1 \qquad (22)$$

while, the sign function (Fig. 2(b)) is expressed by;

$$\text{sgn}(S) = \begin{cases} +1 & \text{when } S > 0 \\ -1 & \text{when } S < 0 \end{cases} \qquad (23)$$

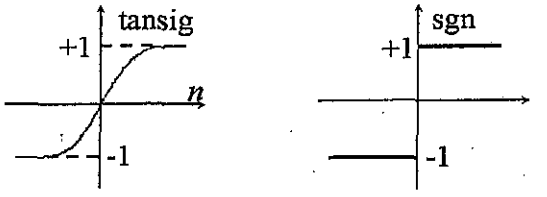


(a) Continuous (sigmoid) (b) Discontinuous (sign)

**Fig. 2** Switching Functions

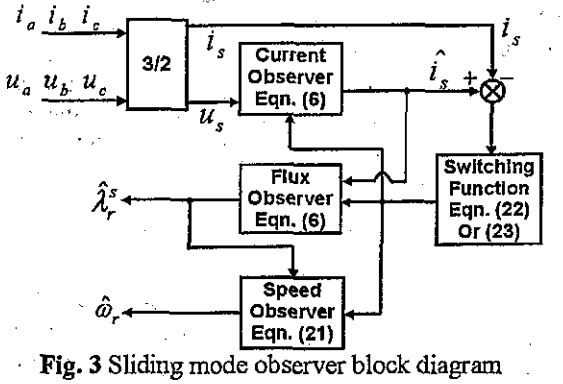


**Fig. 3** Sliding mode observer block diagram

## 5. SYSTEM IMPLEMENTATION

The proposed SMO speed estimation algorithm is implemented and investigated by simulation and experiments. A schematic diagram for the experimental system is shown in Fig. 4. It consists of an induction motor interfaced with a Digital Signal Processor (DSP) (TMS320C31) board for speed estimation. The induction motor is coupled with a dc generator for mechanical loading. The rating and parameters of the induction motor are given in the Appendix.

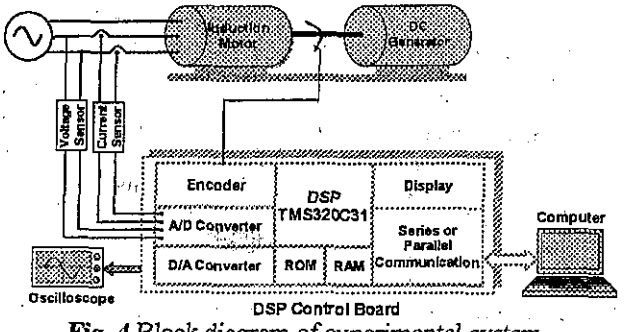


**Fig. 4** Block diagram of experimental system

The system is investigated under operation in real-time in which voltage and current signals are obtained by Hall-effect sensors and sent to the DSP via its A/D input ports. The SMO estimation procedure is implemented by a software program developed on *Matlab/Simulink* and linked to the DSP using a Real Time Interface (RTI) procedure designed for this purpose.

## 6. RESULTS AND DISCUSSION

The main feature intended by the proposed continuous SMO is its ability to obtain a chatter-free system. It has been stated earlier that, the sliding surface is selected to achieve desired system dynamics. The suitability of the chosen sliding surface and the effect of introducing a continuous switching function are firstly examined. Figure 5 shows the sliding surface of SMO, defined by Eqn. 8, with both discontinuous and continuous switching functions. The chattering is clear with discontinuous switching function; however it is almost eliminated with the proposed sigmoid continuous one. This illustrates the effectiveness of using sigmoid switching function to eliminate chattering problem.

Figure 6 shows the phase-plane plot representing the estimated speed signal and its derivative. The plot illustrates the convergence of the estimated speed trajectory with zero speed estimation error at steady state. Thus, the chosen sliding surface exhibits a chatter-free system with the proposed continuous SMO.

The system response is tested to show the effectiveness of the proposed SMO speed estimation algorithm. Both the discontinuous and proposed continuous switching functions are used throughout the study. Results are presented for the conditions of motor starting and load changes.

Experimental results at start up for the discontinuous switching function are shown, respectively, in Fig. 7, while the corresponding results of the continuous switching function are shown, in Fig. 8. For the discontinuous switching function, Fig. 7 shows the experimentally measured and estimated speed signals as well as the speed estimation error. The results show a good agreement between measured and estimated speed signals, however there is high frequency oscillations in the estimated speed which is clearly shown by the speed estimation error. These oscillations are termed as *chattering* phenomenon, which is undesirable and should be eliminated.

For the continuous switching function, Fig. 8 shows the experimentally measured and estimated speed signals as well as the speed estimation error. The results also show a good agreement between measured and estimated speed signals; besides the high frequency oscillations encountered in the last system disappeared. The estimated speed and speed estimation error signals are almost chatter-free. The speed estimation error is quite zero soon after 0.05 sec from starting, this illustrates the high accuracy of proposed speed estimation procedure. The results show the effectiveness of the proposed continuous

switching function for eliminating high frequency oscillations and chattering associated with discontinuous SMO.

Robustness is one of the most distinguished properties of SMO. This property is examined for the proposed SMO to assure that the sigmoid continuous switching function preserves its robustness property. Load torque variations are used for this purpose. Figure 9 shows the experimentally measured and estimated speed signals as well as the speed estimation error for a 50% increase of load torque with a discontinuous switching function. Figure 10 shows the corresponding results with sigmoid continuous function. The system is tested also under load decrease. Figure 11 shows the experimentally measured and estimated speed signals as well as the speed estimation error for a 50% decrease of load torque with a discontinuous switching function. Figure 12 shows the corresponding results with sigmoid continuous function.

Investigating the estimated speed signals and speed estimation error of SMO under load torque variations with both types of switching functions shows clear speed oscillations existing with discontinuous function. Speed estimation error with this type is around 1 rad/sec (3.2%), while it is less than 0.5 rad/sec and decays rapidly to zero after 0.05 sec with the proposed SMO. Both systems exhibit a good robustness and speed estimation accuracy under load torque variations: however the proposed SMO with sigmoid function has another advantage of being a chatter-free.

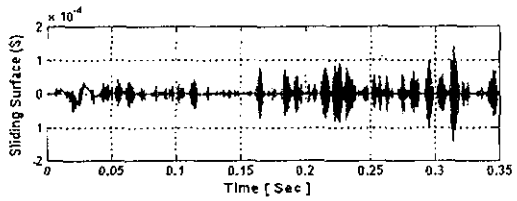


(a) With discontinuous switching function

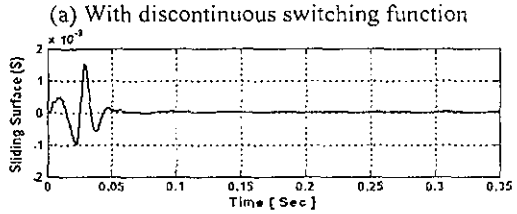


(b) With continuous switching function

**Fig. 5** Sliding surface

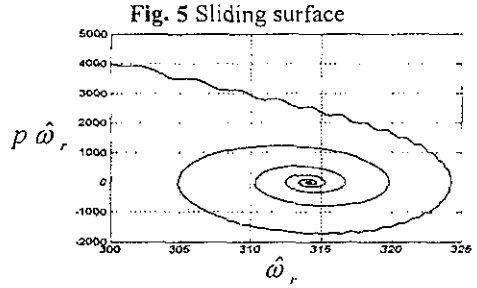


**Fig. 6** phase plane ( $p\hat{\omega}_r - \hat{\omega}_r$ )

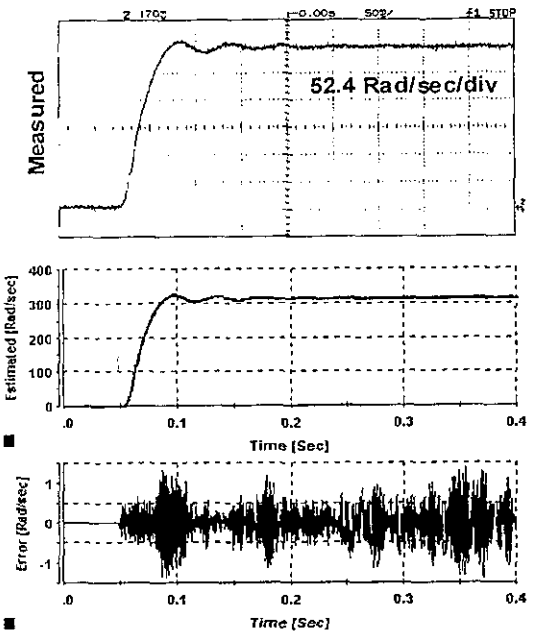


**Fig. 7** Experimental results of measured and estimated speed signals during start-up with discontinuous switching function

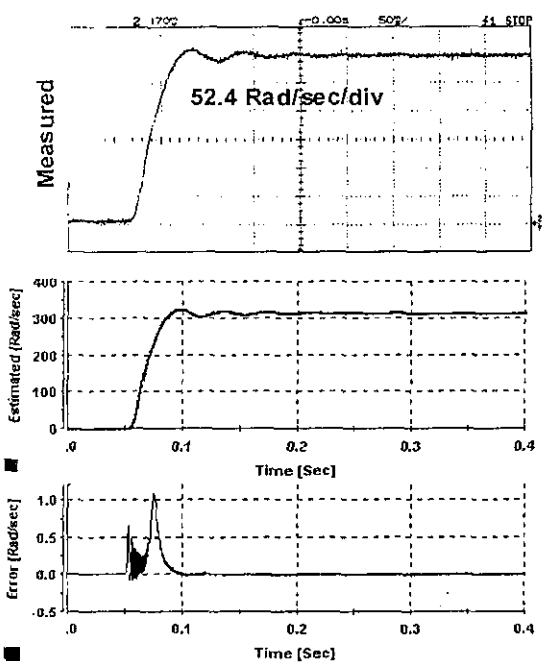


**Fig. 8** Experimental results of measured and estimated speed signals during start-up with continuous switching function

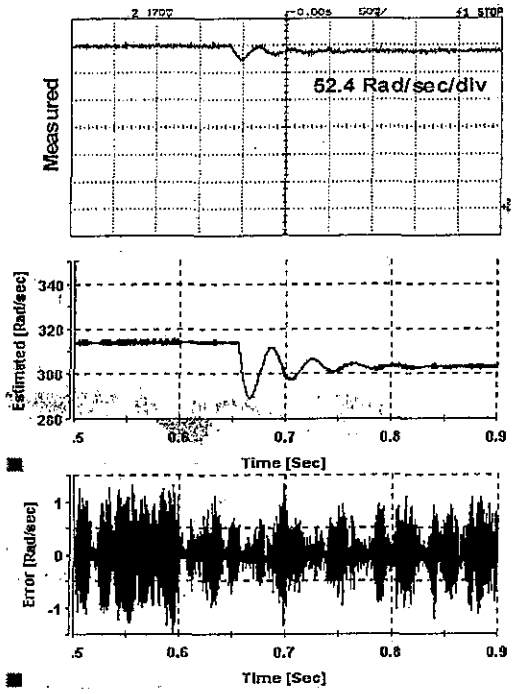


Fig. 9 Experimental results of measured and estimated speed signals at 50% increasing load torque with discontinuous switching function

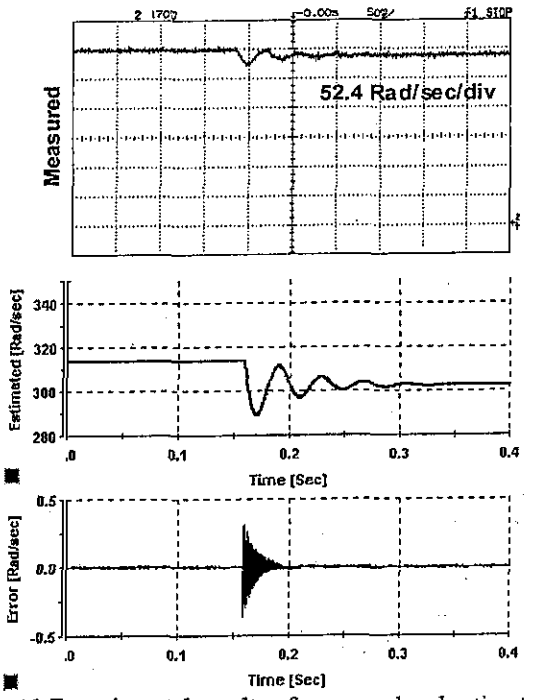


Fig. 10 Experimental results of measured and estimated speed signals at 50% increasing load torque with continuous switching function

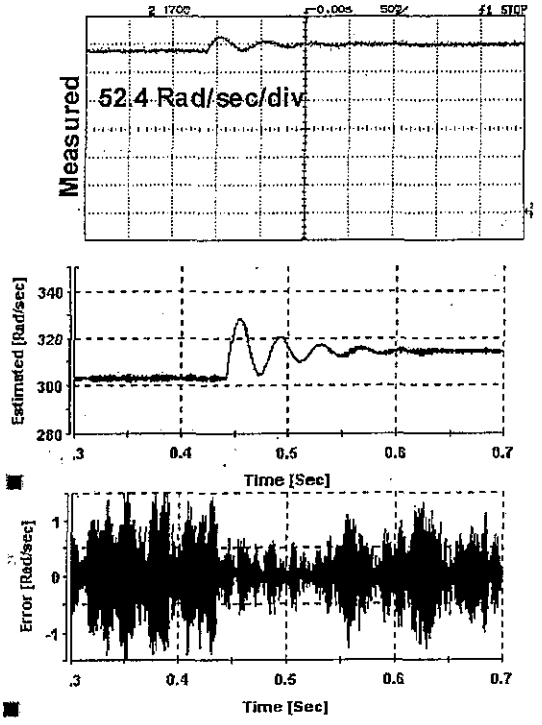


Fig. 11 Experimental results of measured and estimated speed signals at 50% decreasing load torque with discontinuous switching function

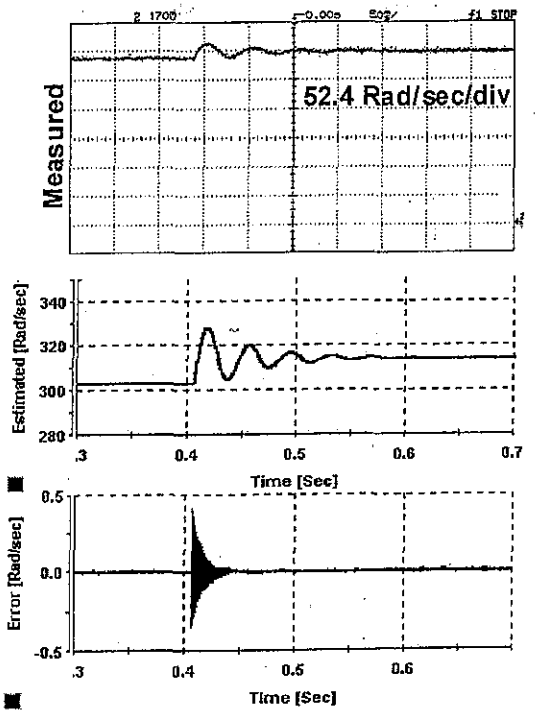


Fig. 12 Experimental results of measured and estimated speed signals at 50% decreasing load torque with continuous switching function

## 7. CONCLUSION

A modified SMO has been introduced to eliminate the chattering phenomenon associated with conventional SMO. The discontinuous switching function has been replaced by a sigmoid continuous one. The measured and estimated speed signals have been in a good convergence at different operating conditions. The system has been examined to show the effectiveness of the proposed SMO for eliminating chattering phenomenon. The analytical and experimental results show high accuracy and robustness of speed estimation with a minimum estimation error that dies out soon after any dynamic variation. A considerable reduction of switching oscillations has also been obtained with the proposed continuous SMO. The proposed SMO speed estimation system has been realized on a Digital Signal Processor (DSP) TMS320C31 platform and experimentally tested in real time.

## 8. REFERENCES


[1] Joachim Holtz, "Sensorless control of induction motor drives" IEEE Proc., Vol. 90, No. 8, August 2002, pp. 1359-1394.

[2] Chul-Woo Park and Woo-Hyen Kwon, "Simple and robust speed sensorless vector control of induction motor using stator current based MRAC," Electric Power Systems Research, Elsevier, Vol. 71, 2004, pp. 257–266.

[3] G. Garcia Soto, E. Mendes and A. Razek, "Reduced-order observers for rotor flux, rotor resistance and speed estimation for vector controlled induction motor drives using the extended Kalman filter technique," IEE Proc.-Electr. Power Applicat., Vol. 146. No. 3, May 1999, PP. 282-288.

[4] Surapong Suwankawin and Somboon Sangwongwanich, "Design strategy of an adaptive full-order observer for speed-sensorless induction-motor drives—tracking performance and stabilization," IEEE Trans. on Ind. Electr., Vol. 53, No. 1, February 2006, pp. 96-119.

[5] Miroslaw Wlas, Zbigniew Krzemin´ski, Jarosław Guzin´ski, Haithem Abu-Rub, and Hamid A. Toliyat, "Artificial-neural-network-based sensorless nonlinear control of induction motors," IEEE Trans. on Energy Conversion, Vol. 20, No. 3, September 2005, pp. 520-528.

[6] S. Xepapas, A. Kaletsanos, F. Xepapas and S. Manias, "Sliding-mode observer for speed-sensorless induction motor drives," IEE Proc. Control Theory Applicat., Vol. 150, No. 6, November 2003, pp. 611-617.

[7] Cristian Lascu and Andrzej M. Trzynadlowski, "Combining the principles of sliding mode, direct torque control, and space-vector modulation in a high-performance sensorless AC drive," IEEE Trans. Ind. Applicat., Vol. 40, No. 1, January/February 2004, pp. 170–177.

[8] Cristian Lascu, Ion Boldea, and Frede Blaabjerg, "Direct torque control of sensorless induction motor drives: a sliding-mode approach," IEEE Trans. Ind. Applicat., Vol. 40, No. 2, March/April 2004, pp. 582-590.

[9] Sang-Min Kima, Woo-Yong Hanb, and Sung-Joong Kima, "Design of a new adaptive sliding mode observer for sensorless induction motor drive," Electric Power Systems Research, Elsevier, Vol. 70, 2004, pp. 16–22.

[10] John Y. Hung, Weibing Gao, and James C. Hung, "Variable structure control: a survey," IEEE Trans. on Ind. Electr., Vol. 40, No. 1, February 1993, pp. 2-22.

[11] Vadim I. Utkin, " Sliding mode control design principles and applications to electric drives," IEEE Trans. on Ind. Electr., Vol. 40, No. 1, February 1993, pp. 23-36.

[12] Adnan Derdiyok, "Speed-sensorless control of induction motor using a continuous control approach of sliding-mode and flux observer," IEEE Trans. on Ind. Electr., Vol. 52, No. 4, August 2005, PP. 1170-1176.

[13] Gregor Edelbaher, Karel Jezernik, and Evgen Urlep, "Low-speed sensorless control of induction machine," IEEE Trans. on Ind. Electr., Vol. 53, No. 1, February 2006, PP. 120-129.


## APPENDIX

### A. List of symbols

| | | | |
|---|---|---|---|
| $L_m$ | Mutual inductance | $\sigma$ | Leakage coefficient |
| $L_r$ | Rotor leakage inductance | $T_e$ | Electromagnetic torque |
| $L_s$ | Stator leakage inductance | $T_L$ | Load torque |
| $R_s$ | Stator resistance | B | Friction coefficient |
| $T_r$ | Rotor time constant | J | Moment of inertia |
| $\omega_r$ | Rotor angular speed | | |

$i_s^s = [i_{ds}^s \quad i_{qs}^s]^T$ Stator current vector

$\hat{i}_s^s = [\hat{i}_{ds}^s \quad \hat{i}_{qs}^s]^T$ Estimated Stator current vector

$\lambda_r^s = [\lambda_{dr}^s \quad \lambda_{qr}^s]^T$ Rotor flux vector

$\hat{\lambda}_r^s = [\hat{\lambda}_{dr}^s \quad \hat{\lambda}_{qr}^s]^T$ Estimated rotor flux vector

$u_s^s = [u_{ds}^s \quad u_{qs}^s]^T$ Stator voltage vector

$\hat{\omega}_r$ Estimated rotor speed

$p = d/dt$ Differential operator

$$a_{11} = aI, \quad a_{12} = cI + dJ, \quad a_{21} = eI, \quad a_{22} = -\varepsilon a_{12}, \quad b_1 = bI$$

$$I = \begin{bmatrix} 1 & 0 \\ 0 & 1 \end{bmatrix}, \quad J = \begin{bmatrix} 0 & -1 \\ 1 & 0 \end{bmatrix}$$

$$a = -\left(\frac{R_s}{\sigma L_s} + \frac{L_m^2}{\sigma L_s T_r L_r}\right), \quad c = \frac{1}{\varepsilon T_r}, \quad d = \frac{\omega_r}{\varepsilon}, \quad e = \frac{L_m}{T_r}$$

$$\varepsilon = \frac{\sigma L_s L_r}{L_m}, \quad b = \frac{1}{\sigma L_s}, \quad \sigma = 1 - \frac{L_m^2}{L_s L_r}, \quad T_r = \frac{L_r}{R_r}$$

### B. Induction motor parameters:-

| | | | |
|---|---|---|---|
| Rated power (w) | 250 | $R_s$ (p.u) | 0.0658 |
| Rated voltage (volt) | 380 | $R_r$ (p.u) | 0.0485 |
| Rated current (Amp.) | 0.5 | $L_s$ (p.u) | 0.6274 |
| Rated frequency (Hz) | 50 | $L_r$ (p.u) | 0.6274 |
| Number of poles | 4 | $L_m$ (p.u) | 0.5406 |